ANALYTIC EVALUATION OF RADIAL STRESSES IN UNFOLDING FAILURE OF COMPOSITE MATERIALS. COMPARISON WITH NUMERICAL SOLUTIONS.

J. M. González-Cantero*[1], E. Graciani[1], A. Blázquez[1], F. París[1]

[1] *Grupo de Elasticidad y Resistencia de Materiales, Universidad de Sevilla, Camino de los Descubrimientos s/n, 41092 Sevilla, Spain*

* *Corresponding Author: jugoncan@yahoo.es*

Keywords: Unfolding Failure, Curved Beam, Composite Materials, Interlaminar Stresses

Abstract

Typical analysis of composite laminates do not consider interlaminar stresses, being considered as negligible in most cases. These stresses are more significant in the case of a curved beam, where Lekhnitskii's equations are typically used for their calculation. However, Lekhnitskii's equations are only exact in the case of an homogeneous anisotropic material, and composite laminates are typically composed of orthotropic laminas with different orientations. A novel calculation method for evaluating stresses in composite curved beams is introduced in this paper and compared with numerical results to show its accuracy.

1. Introduction

The classical laminate theory (see [1], Chapter 4) lets us to calculate in-plane stresses in a plane laminate under bending moments and axial forces, interlaminar stresses being considered negligible. This theory has been applied also to curved beams (see [2]), but the theory is not capable of calculating interlaminar stresses. However, when the laminate is curved with $t \sim R$ (where t is the thickness of the laminate and R the medium radius) interlaminar stresses are higher and become the main failure cause in many cases.

The exact solution in a plane state of a curved beam under a bending moment and axial and shear forces was given by Lekhnitskii et al (see [3], Chapter 3) in the case of an anisotropic homogeneous material. In composite laminates the beam is not homogeneous due to the stacking sequence and it can be an important factor in the maximum value of the interlaminar stresses.

Previous authors have analysed numerically the curved layered beam, see Wisnom [4], and developed 2D in-plane numerical methods that calculate also out-plane stresses, as Robbins Jr. [5].

An analytic model to obtain interlaminar stresses in a curved beam is developed in [6]. That model is compared in this paper with numerical results to show its accuracy. A curved beam with constant radius R under a distribution of axial force $N(\theta)$, shear force $Q(\theta)$ and bending moment $M(\theta)$ is considered as seen in figure 1.

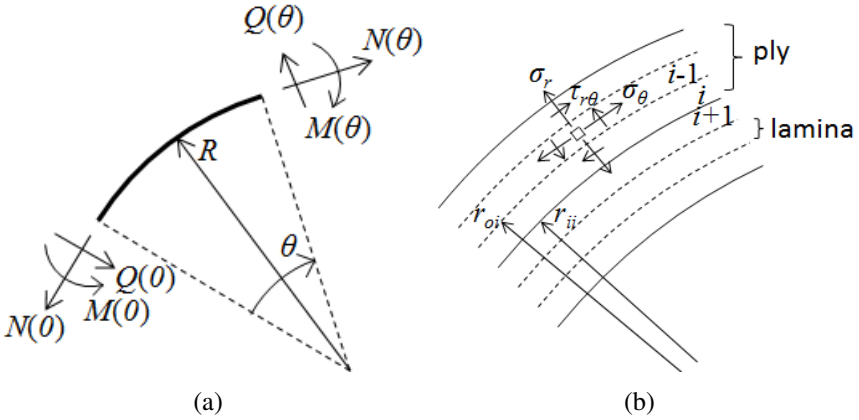

Figure 1. (a) Definition of axial and shear forces and bending moment in a curved beam. (b) Definition of the physical plies and the mathematical laminas.

A cylindrical coordinate system with the radius r and the angle θ in the plane of figure 1 and the axis z perpendicular to the plane is considered.

The model employed to obtain the radial, circumferential and shear stresses in a composite material of N_l plies consists on considering every ply composed of M_l laminas (which are only a mathematical tool without physical meaning, shown in fig. 1), solving the equilibrium, behaviour and compatibility equations for every lamina and taking the limit when $M_l \to \infty$. The problem is simplified supposing a beam model in each lamina, not considering the shear deformation, what is equivalent to approximate displacements in every lamina by the displacements obtained in the homogeneous equivalent material.

Moreover, the problem considered is two-dimensional, and applying the beam approximation in every lamina it becomes a unidimensional problem in each lamina. The unidimensional behaviour equation relating the deformation ε_θ and the circumferential stress σ_θ is given by the stiffness Q^i in the i-th ply: $\sigma_\theta = Q^i \varepsilon_\theta$. This stiffness can be usually approximated applying plane deformation in z and plane stress along the through-thickness direction r.

The stress distributions obtained under these hypotheses are given by [6]:

$$\sigma_\theta^i(r,\theta) = \frac{N_l R(EA)_i}{Wtr}\left(\frac{N(\theta)}{EA} - \frac{M(\theta)}{EV} + (r-R)\left(\frac{M(\theta)}{EI} - \frac{N(\theta)}{EV}\right)\right) \tag{1}$$

$$\tau_{r\theta}^i(r,\theta) = \tau_{r\theta}^{i-1}(r_{oi},\theta)\left(\frac{r_{oi}}{r}\right)^2 + \frac{N_l R(EA)_i}{Wtr} Q(\theta)\left(\left(\frac{1}{EA} + \frac{2R}{EV} + \frac{R^2}{EI}\right)\left(1 - \frac{r_{oi}}{r}\right) + \right.$$
$$\left. + \frac{r_{oi}^2 - r^2}{2r}\left(\frac{1}{EV} + \frac{R}{EI}\right)\right) \tag{2}$$

$$\sigma_r^i = \sigma_{r,M}^i + \sigma_{r,N}^i \tag{3a}$$

$$\sigma^i_{r,M}(r,\theta) = \sigma^{i-1}_{r,M}(r_{oi},\theta)\frac{r_{oi}}{r} - \frac{N_l R(EA)_i M(\theta)}{WtrEI}\left[r_{oi} - r - \left(R + \frac{EI}{EV}\right)\log\left(\frac{r_{oi}}{r}\right)\right] \tag{3b}$$

$$\sigma^i_{r,N}(r,\theta) = \sigma^{i-1}_{r,N}(r_{oi},\theta)\frac{r_{oi}}{r} + \frac{d\tau^{i-1}_{r\theta}(r_{oi},\theta)}{d\theta}\frac{r_{oi}}{r}\left(\frac{r_{oi}}{r} - 1\right) - \frac{N_l R(EA)_i N(\theta)}{Wtr}\left[-R\log\left(\frac{r_{oi}}{r}\right)\left(\frac{1}{EV} + \frac{R}{EI}\right) + \right.$$
$$\left. + \frac{1}{2}(r_{oi} - r)\left(\frac{R}{EI} - \frac{1}{EV}\right) + \left(\frac{r_{oi}}{r} - 1\right)\left(\frac{1}{EA} + \frac{2R - \frac{r_{oi}}{2}}{EV} + \frac{R^2 - \frac{Rr_{oi}}{2}}{EI}\right)\right] \tag{3c}$$

The stiffnesses EA, EI and EV are given by:

$$EI = \frac{\Delta}{A}W \quad ; \quad EV = \frac{\Delta}{B}W \quad ; \quad EA = \frac{\Delta}{D}W \quad ; \quad \Delta = AD - B^2 \tag{4}$$

$$A = \sum_{i=1}^{N_l}\left(Q^i R\log\left(\frac{R + x_i}{R + x_{i-1}}\right)\right) \tag{5a}$$

$$B = \sum_{i=1}^{N_l}\left(Q^i R\left(x_i - x_{i-1} - R\log\left(\frac{R + x_i}{R + x_{i-1}}\right)\right)\right) \tag{5b}$$

$$D = \sum_{i=1}^{N_l}\left(Q^i R\left(R^2\log\left(\frac{R + x_i}{R + x_{i-1}}\right) + \frac{x_i}{2}(x_i - 2R) - \frac{x_{i-1}}{2}(x_{i-1} - 2R)\right)\right) \tag{5c}$$

where $x_i = r_{oi} - R$, $x_{i-1} = r_{ii} - R$, r_{oi} is the outer radius of the ply i and r_{ii} is the inner radius. The stiffness $(EA)_i$ is the equivalent to EA but in a ply instead of the complete beam, given by:

$$(EA)_i = Wt_l Q^i \tag{6}$$

where W is the width of the beam (in the cylinder axis direction), t the thickness of the complete beam and t_l the thickness of a single ply.

The shear $\tau^i_{r\theta}$ and radial σ^i_r stresses in lamina i depends on the stresses in the lamina $i - 1$, so it is necessary to initialize them with a boundary condition given by:

$$\tau^0_{r\theta}(r_{o1},\theta) = \sigma^0_{r,M}(r_{o1},\theta) = \sigma^0_{r,N}(r_{o1},\theta) = 0 \tag{7}$$

2. Comparison with Lekhnitskii's equations

The model can be applied to an homogeneous material considering only one ply, so $(EA)_i = EA$. In this kind of material Lekhnitskii's equations (see [3], Chapter 3) can be applied. Typically

the Lekhnitskii parameter $\kappa = \sqrt{\frac{E_\theta}{E_r}}$ in a composite material is between 1 (isotropic material) and 4.

A comparison between the stresses due to the different efforts obtained from the model applied in an homogeneous material and from Lekhnitskii's equations is represented in the figures 2-4, where a specimen with $t = 3$ mm and $R = 6.5$ mm has been chosen.

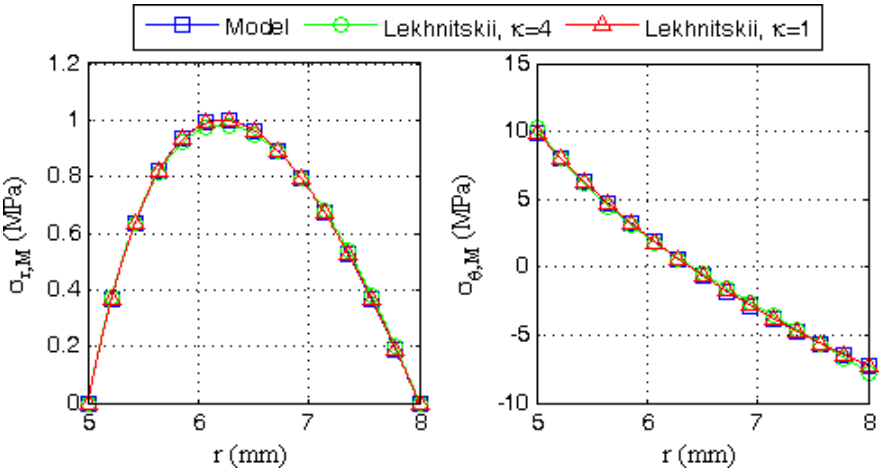

Figure 2. Stresses due to the bending moment $M(\theta)$.

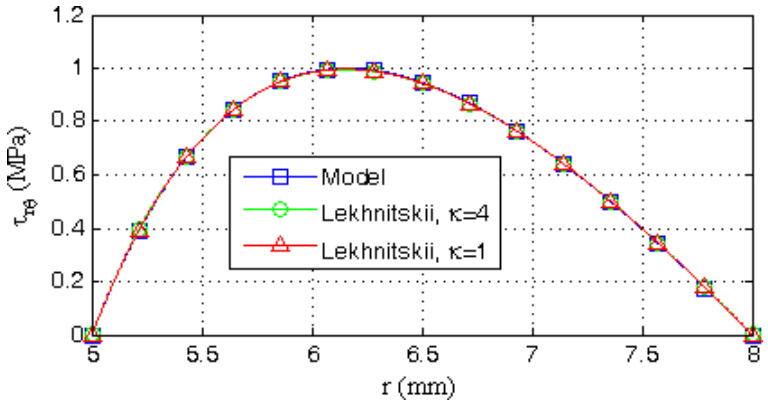

Figure 3. Stresses due to the shear force $Q(\theta)$.

Figure 2 shows the radial stresses $\sigma_{r,M}$ (left) and the circumferential stresses $\sigma_{\theta,M}$ (right) due to the bending moment $M(\theta)$. Figure 3 shows the shear stresses $\tau_{r\theta}$ due to shear force. Both figures shows the high accuracy of the model in a homogeneous material with the range of values of κ considered.

Figure 4 shows the radial stresses $\sigma_{r,N}$ (left) and the circumferential stresses $\sigma_{\theta,N}$ (right) due to axial force. In that case the effect of the variation of κ is higher. As the model does not depend on the value of κ results are less accurate. It can be seen that the accuracy is higher in the case of $\kappa = 1$.

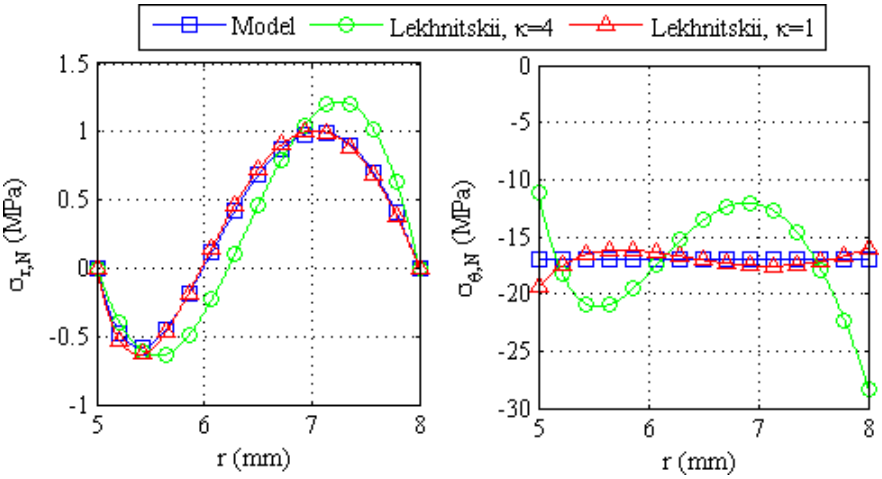

Figure 4. Stresses due to the axial force $N(\theta)$.

3. Comparison with numerical results

Once model equations have been verified in an homogeneous material composite laminates are studied comparing them with numerical results.

3.1. Numerical model

The bar has been modelled in a commercial finite elements code (see [7]) as a 2D problem with shell elements. The load is applied far enough to the interest zone in which stresses are observed so it does not influence the results. At the opposite side of the curved beam the circumferential displacements are prescribed.

Figure 5 shows the force and the moment applied in the free end, that correctly calculated let to obtain the desired stresses in a specific section. If the moment is $M = Ph_1$ the section $\theta = 0$ is only under shear effort, so stresses due to the shear force are obtained in this section. If the moment is $M = Ph_2$ stresses due the axial force are observed in $\theta = \pi/2$. Finally, if $P = 0$ stresses due to the bending moment are observed in any section far enough from the load application point.

Two kind of specimens are considered:

- **Specimen 1:** Stacking sequence: $[45, -45, [90]_3, -45, 45, [0]_2, [45, -45]_2, 0, [45, -45]_5]_S$, Ply properties: $E_{11}/E_{22} = 20.22$, $t = 8.8$ mm, $R = 15.6$ mm.
- **Specimen 2:** Stacking sequence: $[45, 0, -45, 90]_{3S}$, Ply properties: $E_{11}/E_{22} = 20.22$, $t = 8.8$ mm, $R = 15.6$ mm.

The 90º direction is the cylinder axis direction z and the 0º the circumferential direction θ. The first specimen has been chosen as it is an example where Lekhnitskii's equations do not estimate well the maximum value of the radial stresses. The second specimen has been chosen as it is an example where Lekhnitskii's equations do not estimate well the radial failure point.

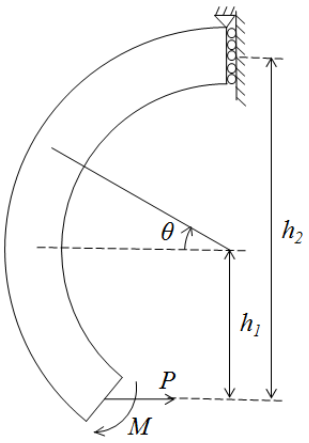

Figure 5. Geometry and loads in the numerical model.

3.2. Results

Several results obtained applying the analytic model, Lekhnitskii's equations and the numerical model to the previous specimens are represented in figures 6-10.

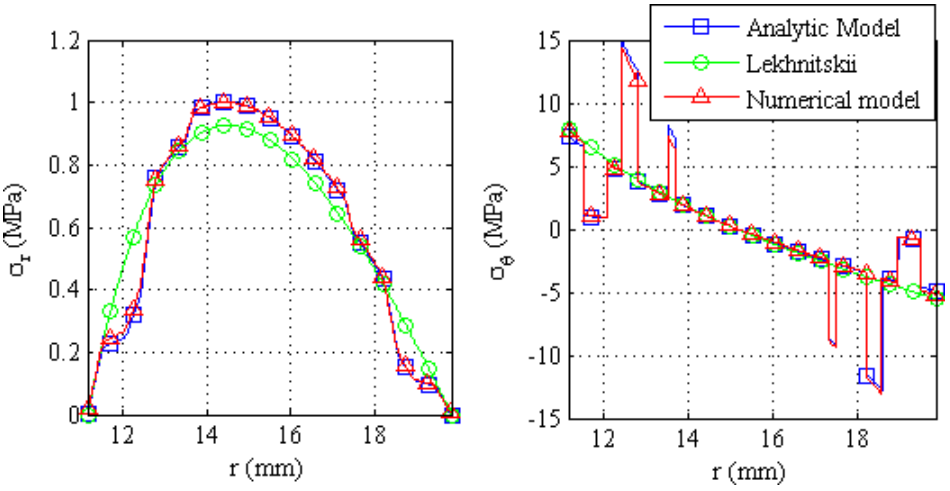

Figure 6. Specimen 1, stresses due to the bending moment.

Figures 6 and 7 show the stresses due to the bending moment in specimens 1 and 2 respectively, where the high accuracy of the analytic method over the numerical results is observed. Moreover they show the capacity to get the stacking sequence dependence of the maximum value of the radial stresses. In specimen 1 the maximum value of the radial stress is a 10% higher that in the Lekhnitskii distribution

Figure 8 show that shear stresses due to the shear force have a similar distribution shape that the radial stresses due to the bending moment, and they are more or less as accurate as that.

Finally, figures 9 and 10 show that the stresses due to the axial force are not so accurate compared with the numerical results. The maximum value of the radial stresses in this cases may have an error even of 100%.

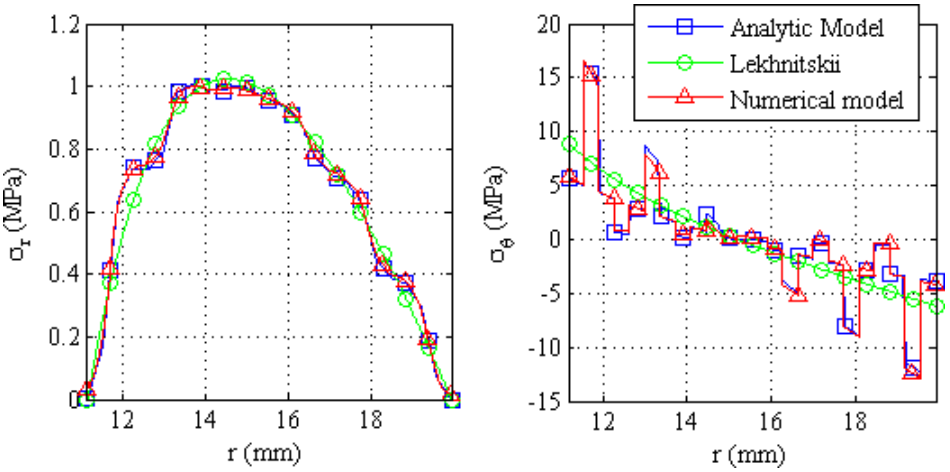

Figure 7. Specimen 2, stresses due to the bending moment.

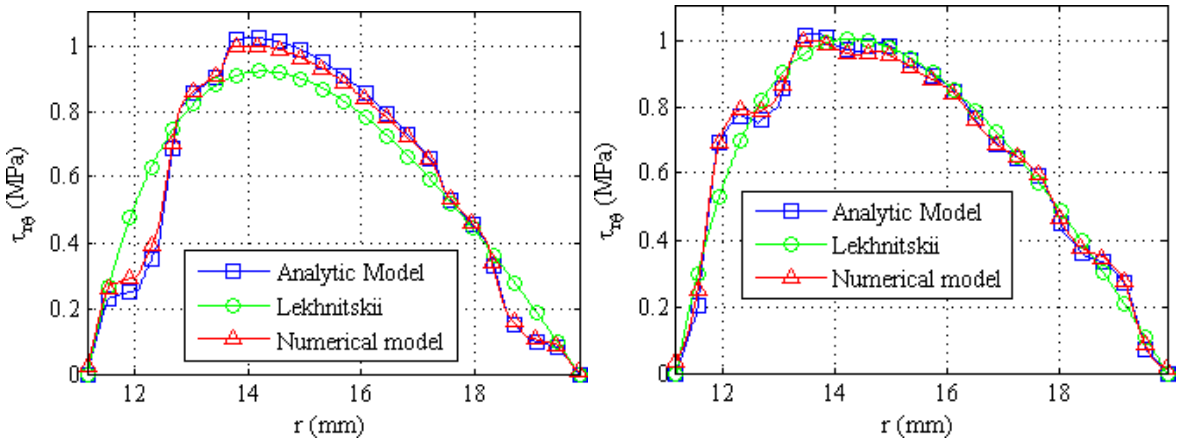

Figure 8. Specimen 1 (left) and Specimen 2 (right), stresses due to the shear force.

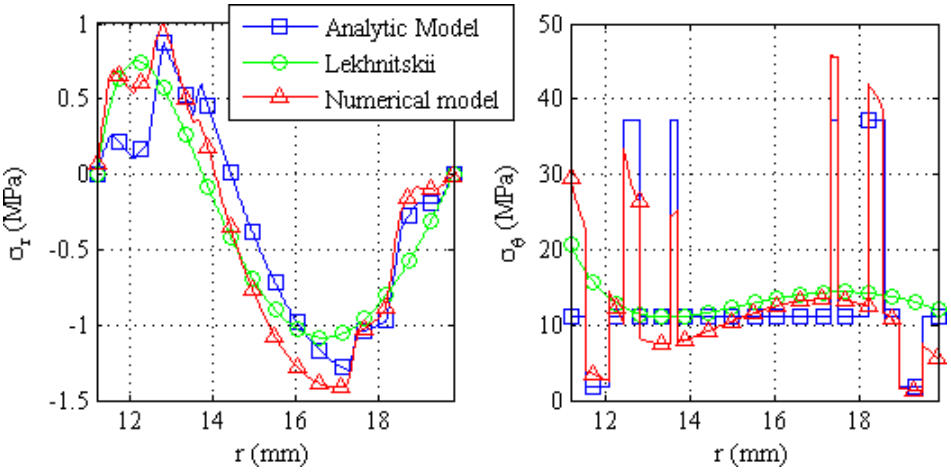

Figure 9. Specimen 1, stresses due to the axial force.

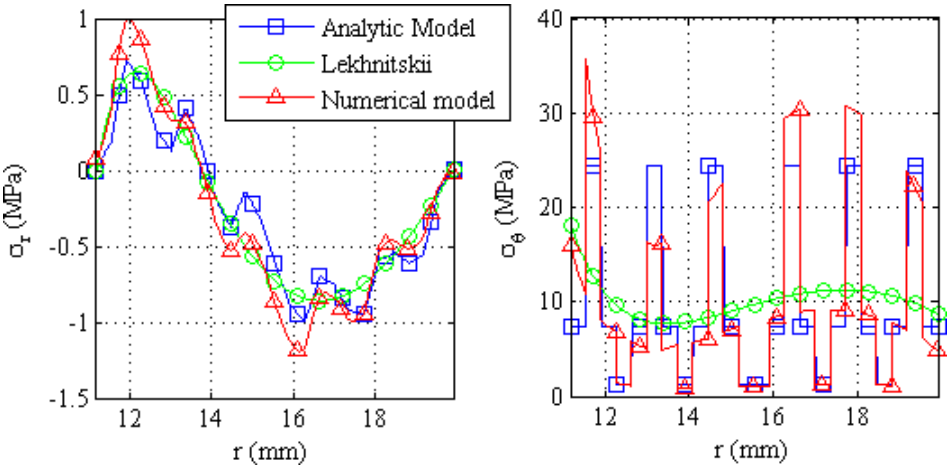

Figure 10. Specimen 2, stresses due to the axial force.

4. Concluding remarks

The method developed in [6] lets us to calculate in a very accurate way the circumferential, radial and shear stresses due to the bending moment and the shear force in a curved beam with constant radius, and the stresses due to the axial force with a higher error.

Nevertheless, the lack of accuracy in the axial force stresses is not important because when an axial force in a curved beam exists it causes a bending moment in another section that induces higher stresses. Therefore the influence of stresses due to the axial force in the failure load is relatively low.

The method is also a powerful tool that allows a stacking sequence optimization which cannot be done with Lekhnitskii's equations.

References

[1] R.M. Jones. *Mechanics of Composite Materials*. Mc Graw-Hill, 1975.

[2] K.C. Lin and C.M. Hsieh. The closed form general solutions of 2-D curved laminated beams of variable curvatures. *Composite Structures*, 79(2007):606–618, 2007.

[3] S.G. Lekhnitskii, S.W. Tsai, and T. Cheron. *Anisotropic Plates*. Gordon and Breach Science Publishers, 1968.

[4] M.R. Wisnom. 3-D finite element analysis of curved beams in bending. *Journal of Composite Materials*, 30(11):1178–1190, 1996.

[5] D.H. Robbins Jr. and J.N. Reddy. Modelling of thick composites using a layerwise laminate theory. *International Journal for Numerical Methods in Engineering*, 36(4):655–677, 1993.

[6] J.M. González-Cantero, E. Graciani, A. Blázquez, and F. París. Evaluation of radial stresses in unfolding failure of composite materials. Analytic model. *In preparation*.

[7] MSC Nastran 2013.1. *Quick Reference Guide*. MSC.Software Corporation, 2013.